

## Intercomparisons of *CloudSat* and Ground-Based Radar Retrievals of Rain Rate over Land

SERGEY Y. MATROSOV

*Cooperative Institute for Research in Environmental Sciences, University of Colorado Boulder, and NOAA/Earth System Research Laboratory, Boulder, Colorado*

(Manuscript received 6 March 2014, in final form 30 July 2014)

### ABSTRACT

Experimental retrievals of rain rates using the *CloudSat* spaceborne 94-GHz radar reflectivity gradient method over land were evaluated by comparing them with standard estimates from ground-based operational S-band radar measurements, which are widely used for quantitative precipitation estimations. The comparisons were performed for predominantly stratiform precipitation events that occurred in the vicinity of the Weather Surveillance Radar-1988 Doppler (WSR-88D) KGWX and KSHV radars during the *CloudSat* overpasses in the vicinity of these ground radar sites. The standard reflectivity-based WSR-88D rain-rate retrievals used in operational practice were utilized as a reference for the *CloudSat* retrieval evaluation. Spaceborne and ground-based radar rain-rate estimates that were closely collocated in space and time were generally well correlated. The correlation coefficients were approximately 0.65 on average, and the mean relative biases were usually within  $\pm 35\%$  for the whole dataset and for individual events with typical rain rates exceeding  $\sim 2 \text{ mm h}^{-1}$ . For events with lighter rainfall, higher biases and lower correlations were often present. The normalized mean absolute differences between satellite- and ground-based radar retrievals were on average  $\sim 60\%$ , with an increasing trend for lighter rainfall. Such mean differences are comparable to combined retrieval errors from both ground-based and satellite radar remote sensing approaches. Evaluation of potential effects of partial beam blockage on the ground-based radar measurements was performed, and the influence of the choice of relation between WSR-88D reflectivity and rain rate that was utilized in the ground-based rain-rate retrievals was assessed.

### 1. Introduction

Although the primary goal of the *CloudSat* nadir-pointing W-band (94 GHz; wavelength  $\lambda = 3.2 \text{ mm}$ ) Cloud Profiling Radar (CPR) is to collect global information on clouds, this spaceborne radar proved to be a useful tool for observing and quantifying precipitation (e.g., Stephens et al. 2008). Traditional nonpolarimetric radar approaches for quantitative precipitation estimation (QPE) are based on relating the equivalent radar reflectivity factor  $Z_e$  (hereinafter, just reflectivity) to rain rate  $R$ . These approaches, however, are of limited use for interpreting *CloudSat* data in liquid precipitation because of a number of factors including high attenuation of W-band signals in rain, multiple-scattering (MS) effects that are due to the geometry of observations

(e.g., Battaglia et al. 2010), and non-Rayleigh-scattering effects, which usually result in saturation of non-attenuated W-band reflectivities in rainfall at a level of  $\sim 25\text{--}27 \text{ dBZ}$  (Matrosov 2007).

*CloudSat* methods for rain-rate estimation have to utilize radar signal-attenuation effects as useful information for liquid precipitation retrievals (e.g., Matrosov et al. 2008; Haynes et al. 2009; Mitrescu et al. 2010; Lebsock and L'Ecuyer 2011). These effects are used with *CloudSat* data in different ways. Most existing methods use the path-integrated-attenuation (PIA) constraint, which is determined by assuming that radar returns from the surface in clear air are known with a reasonable accuracy. Application of the PIA-based retrieval approaches, such as those used to derive the existing *CloudSat* rainfall "2C-PRECIP-COLUMN" (Haynes et al. 2009) and "2C-RAIN-PROFILE" (Lebsock and L'Ecuyer 2011) products, is currently limited to CPR measurements over water, when would-be surface returns in the absence of hydrometeors in a vertical atmospheric

---

Corresponding author address: Sergey Y. Matrosov, R/PSD2, 325 Broadway, Boulder, CO 80305.  
E-mail: sergey.matrosov@noaa.gov

column are approximated on the basis of a priori information about surface wind speed and temperature (e.g., Tanelli et al. 2008). Use of the PIA constraint is not generally available for heavier rainfall when the surface returns are not detected because of a combination of very strong attenuation and MS effects (e.g., Battaglia et al. 2008).

A gradient method to retrieve rain rates from *CloudSat* data (e.g., Matrosov 2007, 2013) estimates the W-band attenuation coefficient (i.e., specific attenuation) in rain from the vertical gradients of observed CPR reflectivities and then relates this coefficient to  $R$ . This method does not use the PIA information from surface returns and therefore is applicable to observations above any surfaces. The main assumption of this method is that after accounting for gaseous attenuation the vertical gradients of observed reflectivities are primarily caused by liquid hydrometeor attenuation and, for heavier rainfall, by MS enhancement. Changes in a vertical profile of nonattenuated reflectivities contribute to the uncertainty of estimates of the attenuation coefficient (and therefore rain rate). Given this assumption, the gradient method is best suited for stratiform precipitation for which vertical variations in nonattenuated reflectivity profiles are relatively small even at centimeter wavelengths (e.g., Bringi and Chandrasekar 2001), which are typically used in ground-based precipitation sensing radars. At W band the vertical variability of nonattenuated reflectivity in stratiform rain is further suppressed relative to longer wavelengths because of strong non-Rayleigh-scattering effects.

The main objective of this study was to evaluate *CloudSat* gradient-method rain-rate retrievals in stratiform rainfall over land using ground-based scanning S-band ( $\sim 3$  GHz) Weather Surveillance Radar-1988 Doppler (WSR-88D) measurements. The WSR-88D data are routinely used over the United States for QPE purposes. The uncertainty of WSR-88D QPE retrievals could be as high as 30%–40% as compared with rainfall accumulations that are directly observed by rain gauges, which are often considered to be the “ground truth” (e.g., Krajewski et al. 2010). Nonetheless, scanning-precipitation-radar-based QPE remains the main remote sensing tool for obtaining precipitation information in many practical applications. Earlier different ground-based radar measurements have been used to validate the *CloudSat* precipitation-occurrence algorithm (Hudak et al. 2008).

## 2. Precipitation events used for intercomparisons

With a few gaps in the western United States, the Next Generation Weather Radar (NEXRAD) network of WSR-88Ds, which have a 460-km nominal “long” range

for reflectivity measurements, covers most of the area of the lower 48 states. Although the WSR-88D systems sample reflectivity data at a 1-km range by  $1^\circ$  azimuth grid in the legacy resolution mode and at a 0.25 km by  $0.5^\circ$  grid in the super resolution mode, which has been in use approximately from the summer of 2008, the actual cross-beam resolution degrades with range because of beam broadening and Earth sphericity effects. The WSR-88D data are collected in repetitive volume patterns, which consist of several azimuthal plan position indicator scans conducted at different elevation angles. A typical duration of a volume pattern is approximately 5 min.

The *CloudSat* CPR resolution volume is  $\sim 1.5$  km across the satellite track,  $\sim 1.8$  km along the track, and 0.5 km in the vertical direction (Tanelli et al. 2008). Vertical oversampling allows for providing vertical profiles of observed reflectivity with an increment of 0.24 km. Overall CPR and WSR-88D sampling volumes near the ground radar sites are not vastly different, which is favorable for comparisons of precipitation-retrieval results. Two consecutive *CloudSat* orbit ground tracks are spaced by  $\sim 24.7^\circ$  in longitude. The orbits approximately repeat themselves each 16-day period.

Validation/evaluation of different remote sensing QPE methods is usually performed on the basis of the best available collocated comparisons of rainfall accumulations over a certain time interval (e.g., for hourly accumulations) or event total accumulations obtained from methods considered. One example of such an evaluation is comparisons of ground-radar-based QPE results with available gauge data (e.g., Krajewski et al. 2010). Meaningful comparisons with gauge accumulations, however, are not practical for *CloudSat* rainfall retrievals (except, maybe, for climatological snowfall comparisons in the polar regions where the ground separation between the orbits is much smaller than in the midlatitudes and tropics) because of such factors as fast satellite orbit speed, the long revisiting time period, a large ground-track separation between consecutive orbits, vastly differing resolution volumes, and the fact that most gauge types (unlike the CPR) are better suited to provide information about rainfall accumulation than about instantaneous rain rates.

Because of the impeding factors stated above, this study focuses on rain-rate comparisons as retrieved from *CloudSat* and WSR-88D measurements with the best possible collocation in space and time. Although WSR-88D-based QPE retrievals are obviously not exactly the ground truth, such comparisons have value because relatively novel *CloudSat* rain-rate retrievals over land are compared with the results from the ground-based

TABLE 1. Statistical parameters characterizing comparisons of *CloudSat* and WSR-88D ( $Z_e = 200R^{1.6}$ ) rain-rate retrievals. Means, standard deviations, and RMSE are in millimeters per hour, and RMB and NMAD are in percent.

Event	Mean WSR-88D <i>R</i> estimate	Std dev of WSR-88D <i>R</i>	Mean CPR <i>R</i> estimate	Std dev of CPR <i>R</i>	<i>r</i>	RMB	RMSE	NMAD
All 12 events	2.1	2.0	2.4	1.9	0.67	10	1.9	58
KGWX								
13 Sep 2007	0.8	0.6	1.2	0.9	0.37	51	1.0	89
16 Jul 2009	1.4	0.7	1.8	0.9	0.42	29	1.1	56
1 Aug 2009	1.9	1.3	2.5	1.7	0.64	32	1.5	67
4 Oct 2009	2.6	2.4	3.1	2.3	0.68	19	2.0	48
16 May 2010	3.8	2.7	2.9	1.6	0.69	-23	2.1	43
9 Aug 2012	2.5	0.9	2.0	1.1	0.41	-20	1.2	37
KSHV								
19 Oct 2006	2.3	2.9	2.9	2.4	0.66	26	2.2	76
7 Jan 2007	3.4	3.2	3.3	2.7	0.60	-3	2.7	58
30 Mar 2008	0.7	0.5	1.2	1.0	0.48	73	1.1	116
27 Oct 2009	1.2	1.5	1.8	2.5	0.63	52	1.6	81
10 Jul 2010	0.6	0.6	1.1	0.8	0.22	87	1.4	93
15 Nov 2010	4.4	2.4	2.9	1.2	0.68	-34	2.2	57

meteorological-radar QPE approach, which has been in practical use for many years and is relatively well established. Realize, however, that instantaneous rain rates generally exhibit higher spatial and temporal variability than do rainfall accumulations.

Intercomparisons of WSR-88D and *CloudSat* CPR retrievals are most practical for precipitation events observed when the satellite crosses over the ground-based radar sites (or over locations in the vicinity of these sites), where ground-based and spaceborne retrievals could be better collocated. *CloudSat* ground tracks pass within a few kilometers of a number of the NEXRAD sites. This study focuses on the precipitation events observed in the vicinity of two WSR-88Ds: the KGWX Greenwood Springs, Mississippi, radar (33.8969°N, 88.3292°W) and the KSHV Shreveport, Louisiana, radar (32.4508°N, 93.8414°W). The site altitudes for these radars above mean sea level (MSL) are approximately 140 and 80 m for KGWX and KSHV, respectively.

The ground-based-radar choice was dictated, in part, by the fact that for such southern locations of the WSR-88D sites the freezing level in the atmosphere is relatively high, even during colder months, allowing for retrieval of rain rates by use of the gradient method, which requires at least several resolution gates that are free of ground clutter and melting-layer contamination. It corresponds to a conservative requirement of freezing-level (FL) heights being approximately 2 km above the radar site because CPR measurements in the first several gates, whose centers are nominally above the ground, could be contaminated by surface returns and because the melting layer in stratiform precipitation systems is approximately 500 m thick (e.g., Matrosov 2008). The relatively

flat terrain around the KGWX and KSHV WSR-88D sites also minimizes influence of radar beam blockage and ground-clutter effects on precipitation observed with the ground-based radars.

*CloudSat* passage over a particular ground-based radar during a precipitation occurrence in the vicinity of that radar site is a relatively rare event. Of main interest to this study were precipitation events that consisted mostly of stratiform-rain regions covering relatively large areas (at least several dozens of kilometers). This situation allows for better collocation of satellite and ground-based retrievals and results in more data points for comparisons. Stratiform rainfall typically produces a radar bright band (BB) that is located just below the freezing level (e.g., Bringi and Chandrasekar 2001). Unlike the BB in longer-wavelength radar observations for which the BB is caused by reflectivity enhancement by melting snow/ice particles, the BB in CPR measurements is caused, in part, by strong signal attenuation in liquid hydrometeors (Sassen et al. 2007; Matrosov 2008).

An examination of the available *CloudSat* overpasses, which occurred over the KGWX radar site during 2006–12, revealed six predominantly stratiform rainfall events, for which horizontal extents along the *CloudSat* ground track exceeded approximately 50 km and FL heights were greater than 2 km. These events, which are typically associated with the passage of frontal atmospheric systems, were observed on the dates shown in Table 1. The *CloudSat* orbit crossings over the vicinity of the KGWX ground-based radar site occur on the ascending satellite node at approximately 1915 UTC. It corresponds to 1415 central daylight time at the site location.

The same number of precipitation events with the same characteristics (i.e., mostly stratiform rainfall with a detectable BB covering a horizontal range that is greater than approximately 50 km in the ground-based-radar coverage area) was observed also when the *CloudSat* crossed over the vicinity of the KSHV radar site during 2006–12. The dates of these KSHV crossings are also shown in Table 1. The KSHV site crossings occur on the descending satellite node. The crossing time is approximately 0820 UTC, which corresponds to nighttime at the KSHV location.

The relatively modest number (i.e., 12) of satellite overpasses in this study is explained by event requirements (i.e., the dominance of the stratiform regime, the spatial extent of precipitation, and the FL height), by the stoppage in *CloudSat* operations during April–October 2011, by the fact that only the orbits above the two WSR-88D locations were considered, and by the relatively long repetition time of the same orbits (i.e., 16 days). On the other hand, these events provided a relatively large amount of individual comparison data points, as shown in section 4. The fact that in general all of the available events that satisfied the requirements mentioned above were considered allows an assumption that the comparisons provided below are representative of mostly stratiform rainfall.

### 3. Intercomparison approaches and a case study

An example of the observed *CloudSat* CPR reflectivity cross section of the KGWX precipitation event that occurred on 4 October 2009 is shown in Fig. 1. The

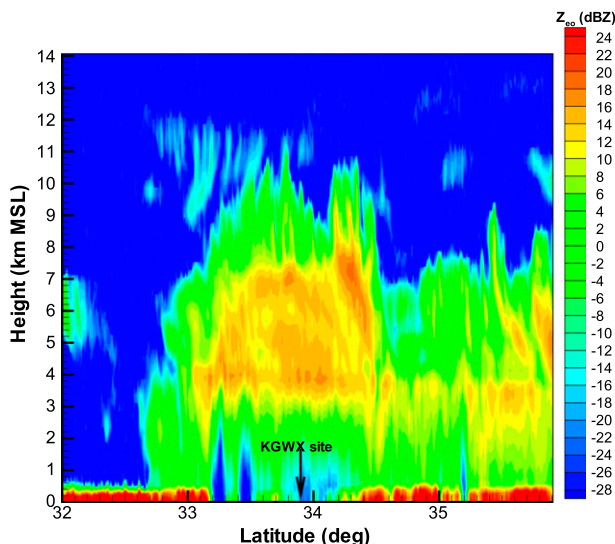


FIG. 1. A cross section of *CloudSat* CPR reflectivity during a precipitating event observed on 4 Oct 2009 (~1915 UTC) in the vicinity of the KGWX WSR-88D site.

satellite ground track passed within 1 km of the KGWX radar. A region of rainfall extends to the both sides from the radar site. Near the KGWX site, the direction of the *CloudSat* orbit extends approximately in south–north direction along the azimuth of 348°. As seen in Fig. 1, the CPR BB features are prominent and are observed at an altitude of about 4 km MSL with a tendency of descending toward the ground as the satellite moves north.

For the precipitation event of 4 October 2009, Fig. 2 shows the *CloudSat* ground track overlaid on the map of

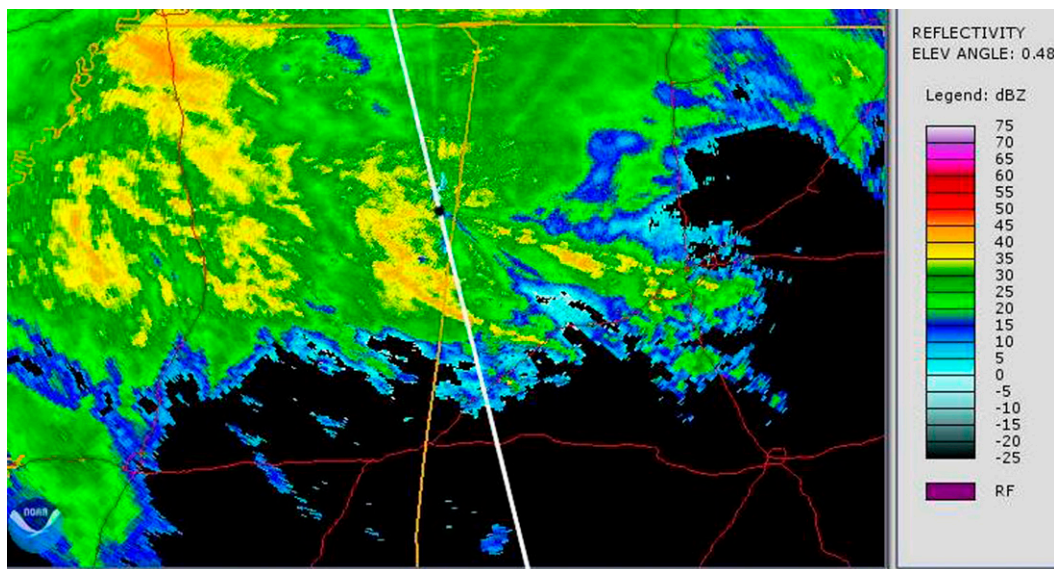


FIG. 2. *CloudSat* ground track (shown by a white line) for 1914 UTC 4 Oct 2009 overlaid on the lowest elevation tilt reflectivities from the KGWX radar, the location of which is shown by the black dot.

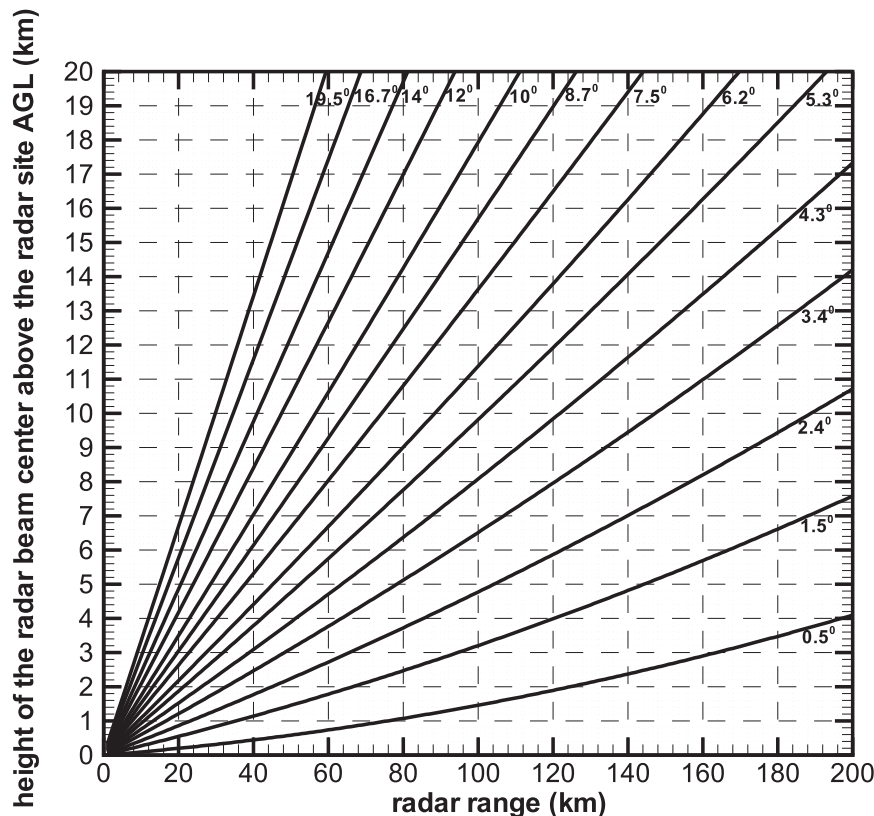


FIG. 3. Heights of the WSR-88D beam centers above ground level for elevation angles employed during VCP-11 scanning.

KGWX radar reflectivity measurements conducted at the lowest beam elevation angle (i.e.,  $0.48^\circ$ ) almost simultaneously with the satellite passage. The sequence of radar beam elevation angles (tilts), which are used for WSR-88D volume scans, is determined by the volume coverage patterns (VCPs). The VCP-11 was typically used for observations of precipitation events analyzed in this study, including the KGWX event of 4 October 2009 shown here in relative detail. This VCP has the best overall volume coverage. WSR-88D scanning during this VCP is performed for a sequence of 14 radar elevation angles  $\beta$ , ranging from  $\sim 0.5^\circ$  to  $19.5^\circ$ . Typical values of the elevation angles for this VCP are shown in Fig. 3. The lowest elevation angle of about  $0.5^\circ$  approximately corresponds to the half beamwidth of the WSR-88D antennas. The radar elevation tilt angles in Fig. 3 represent the average values. The actual beam elevations usually slightly vary for individual volume scans. The heights of the radar beam centers above the radar site level for the VCP-11 elevation angle tilts as a function of the distance from the radar are also shown in Fig. 3. These heights increase with radar range because of Earth sphericity and refraction effects. During some of the experimental events analyzed in this study,

the VCP-12 and VCP-121 were used for WSR-88D scanning instead of the VCP-11. These other VCPs have a slightly different selection of beam elevation tilts (<http://en.wikipedia.org/wiki/NEXRAD>). For all WSR-88D VCPs, however, the lowest and highest beam elevations are  $\sim 0.5^\circ$  and  $19.5^\circ$ , respectively; therefore, the total space coverage is approximately the same.

#### a. The WSR-88D procedure for rain-rate retrieval

The WSR-88D volume-scan measurements can be used to reconstruct S-band reflectivities in different planes emulating horizontal and vertical cross sections. The data from the 1914 UTC KGWX radar volume scan, which closely corresponds to the time of *CloudSat* passage over the radar site shown in Fig. 1, were used to reconstruct the vertical cross section of observed KGWX reflectivities in the vertical plane of CPR measurements. Figure 4 shows this reconstruction of S-band reflectivities, which are practically unattenuated by moderate rain, in the plane of the *CloudSat* reflectivity cross section from Fig. 1. The exact latitude and longitude points of the CPR data were used to interpolate KGWX data presented in Fig. 4. In this figure the wedgelike region of no data just above the radar site,

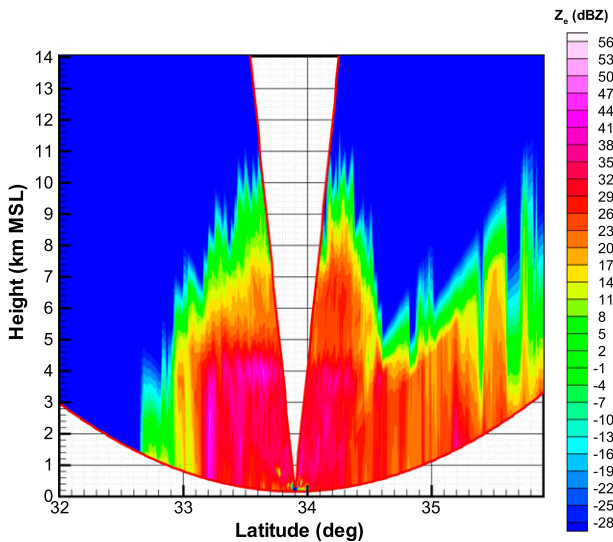


FIG. 4. A cross section of KGWX radar reflectivities matching the *CloudSat* overpass on 4 Oct 2009 that is shown in Fig. 1. The lower and upper lines bounding the areas of no data correspond to the lower/upper edges of the first/last tilts (i.e.,  $0.0^\circ$  and  $20.0^\circ$ ) of the WSR-88D beam.

which is located at 0.14 km MSL, is not sampled by the KGWX radar because the elevation angle tilt is limited by  $19.5^\circ$ .

When reconstructing the WSR-88D reflectivity cross sections, the heights of the upper and lower edges of the radar beam [ $h_i^{(u)}$  and  $h_i^{(l)}$ , respectively] for a given elevation angle  $\beta_i$  (where  $i$  is the beam tilt number) and the radar range were estimated for the spherical Earth geometry using the approach from Doviak and Zrníc (1993, their Eqs. 2.28) and accounting for the NEXRAD radar beamwidth of  $0.96^\circ$  [i.e.,  $h_i^{(u)}$  and  $h_i^{(l)}$  correspond to the elevation angle tilts of  $\beta_i + 0.48^\circ$  and  $\beta_i - 0.48^\circ$ , respectively] with an assumption of the Gaussian antenna pattern. The WSR-88D reflectivity data were sampled at latitudes and longitudes of each *CloudSat* CPR data profile with averaging along the beam of  $\pm 0.9$  km from the profile center. Such averaging approximately accounts for the CPR footprint along the satellite ground track. When sampling the ground-based radar data at CPR data geographical locations, the WSR-88D measurements from two neighboring azimuths that bracket the direction to the center of the CPR profile were linearly interpolated to match better the satellite data.

From comparisons of Figs. 1 and 4, it can be seen that, despite its coarser resolution, the WSR-88D reflectivity cross section reproduces the general vertical features of the precipitating system seen in the CPR data, including higher cloud tops between latitudes of about  $33.2^\circ$  and  $34.5^\circ$ , and some isolated reflectivity spikes (e.g., near

$35.5^\circ$ ). Except the vicinity of the radar site (i.e., approximately between  $33.4^\circ$  and  $34.3^\circ$ ), the radar BB are not very well pronounced in the KGWX data. This can be explained by the beam-broadening effects, which degrade the actual WSR-88D resolution with increasing range. The closely collocated (in space and time) *CloudSat* CPR and KGWX WSR-88D measurements, such as those shown in Figs. 1 and 4, allow for detailed intercomparisons of the spaceborne and ground-based rain-rate retrievals with proper matching satellite and ground-based radar estimates.

Although the NEXRAD network was polarimetrically upgraded during 2012–13 and new dual-polarization radar QPE approaches are being developed, the WSR-88D data collocated with *CloudSat* measurements available to this study include only the WSR-88D reflectivity and Doppler velocity measurements. Therefore, the conventional WSR-88D rain-rate retrievals that are based on S-band reflectivity ( $Z_e$ ) are considered here. Such retrievals are used in the National Mosaic and QPE system (NMQ; e.g., Zhang et al. 2011). The standard NEXRAD  $Z_e$ – $R$  relation for stratiform rainfall, which is given by

$$Z_e (\text{mm}^6 \text{m}^{-3}) = 200R^{1.6} (\text{mm h}^{-1}), \quad (1)$$

was primarily utilized with ground-based WSR-88D measurements in this study.

As mentioned above, the precipitation event shown in Fig. 1 is generally of the stratiform type. For the most part it exhibits a pronounced BB except in an area of warm rain (i.e., at latitudes south from approximately  $33^\circ$ ), which has echo tops that are generally lower than the environmental freezing level. There are also some small regions, where rainfall can be interpreted as convective (e.g., near latitudes of  $33.25^\circ$ ,  $33.35^\circ$ , and  $35.3^\circ$ ). The CPR BB is elevated in these regions (relative to the stratiform areas), which is likely due to some upward air motions. The CPR ground returns are not clearly seen in convective regions, nor in some stratiform areas (e.g., around  $34^\circ$ ), because the W-band signal attenuation by rainfall there is strong and MS effects are significant. Overall, the BB separates the predominantly ice-phase precipitating cloud above and the liquid hydrometeor layer below. The rain-rate retrievals from the WSR-88D were performed using the reflectivity measurements observed when corresponding interpolated resolution volumes were fully within the rainfall layer.

In addition to the spatial interpolation and averaging of the WSR-88D data, the linear time interpolation of the ground-based radar measurements was performed using two consecutive volume scans that bracket the CPR profile time. All of the interpolation/averaging

procedures for the given tilt data as mentioned above were performed for the S-band reflectivity measurements in units of millimeters to the sixth power per meter cubed. Interpolating introduces some uncertainties in WSR-88D reflectivities matched with CPR measurements. These uncertainties might contribute to the scatter in the retrieved rain-rate data, which is analyzed in section 4.

The resulting mean WSR-88D reflectivities were then converted to rain-rate estimates using the  $Z_e$ - $R$  relation. For each CPR profile, the mean NEXRAD derived rain rate  $R_N$  was calculated as an average of all rain rates at elevation tilts that are fully within the rainfall layer. The upper boundary of this layer  $h_r$  was determined using the CPR BB height  $h_{BB}$ :

$$h_r = h_{BB} - 0.6 \text{ km}, \quad (2)$$

where the 0.6-km term conservatively accounts for a thickness of the melting layer, the influence of which should be minimized when calculating WSR-88D rain-rate estimates. The CPR BB heights were used because WSR-88D BBs are often not very pronounced (especially at longer radar ranges) because of the beam-broadening effects.

#### b. The CloudSat procedure for rain-rate retrievals

The *CloudSat* reflectivity-gradient method estimates the W-band attenuation coefficient in rain  $\alpha(h)$  at a height  $h$  from the vertical gradients of measured W-band  $Z_{eo}$  reflectivity as (Matrosov 2007, 2013)

$$\alpha(h) = 0.5[\partial Z_{eo}(h)/\partial h]_{ss} - G_o(h), \quad (3)$$

where the term  $G_o(h)$  accounts for model attenuation in atmospheric gases and nonprecipitating liquid. The subscript *ss* for the gradient denotes the single-scattering-assumption values, which are obtained from the observed-gradients values affected by MS {i.e.,  $[\partial Z_{eo}(h)/\partial h]_{ms}$ } as

$$[\partial Z_{eo}(h)/\partial h]_{ss} = \gamma^{-1}[\partial Z_{eo}(h)/\partial h]_{ms}. \quad (4)$$

In (4) the dimensionless coefficient  $\gamma \leq 1$ , and the values of this coefficient for stratiform rainfall with different FL heights are adopted from Matrosov et al. (2008). Because  $\gamma$  also depends on rain rate, correcting for MS requires iterations.

After estimating the  $\alpha(h)$  and correcting for the air-density height changes, the retrieved *CloudSat* rain-rate values are derived from the linearized relation between rain rate and attenuation coefficient:  $R \text{ (mm h}^{-1}\text{)} = 1.2\alpha \text{ (dB km}^{-1}\text{)}$  (Matrosov 2007). A typical estimated retrieval uncertainty is approximately 30%–40% for rain

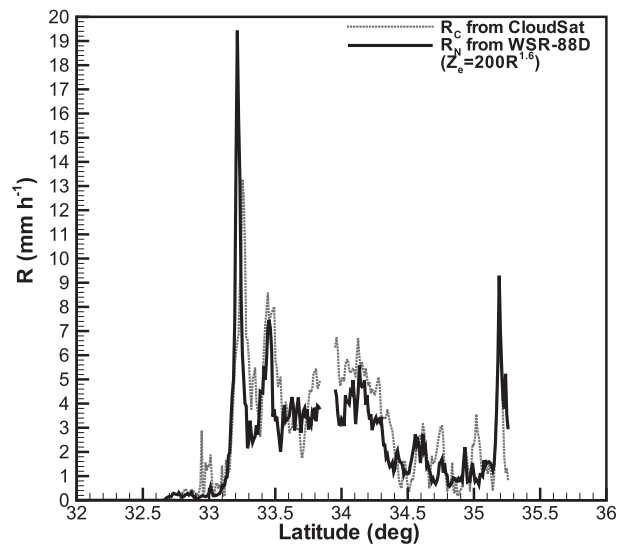


FIG. 5. Rain rate along the satellite-orbit ground track retrieved from CPR and KGWX WSR-88D measurements during the *CloudSat* overpass at 1914 UTC 4 Oct 2009.

rates between approximately 5 and 15  $\text{mm h}^{-1}$ , and it increases for lower rain rates. Multiple scattering overwhelms *CloudSat* measurements for heavy rainfall, and retrievals of rain rates that are higher than about 20–25  $\text{mm h}^{-1}$  using any *CloudSat* method are problematic.

#### c. Intercomparisons for the case study

For the event of 4 October 2009, Fig. 5 shows WSR-88D rain rates  $R_N$  sampled along the *CloudSat* ground track according to the procedures described above. The data are not shown for latitudes that correspond to the KGWX radar ranges when the upper edges of the lowest tilt WSR-88D beam were higher than the upper boundary of the rain layer [i.e.,  $h_1^{(u)} > h_r$ ]. For those latitudes, WSR-88D-based rainfall QPE is contaminated by melting and ice hydrometeors. The comparison data affected by the so-called QPE cone of silence (see Fig. 4) near the radar site, within which no WSR-88D data are available because of the tilt limitations, were excluded.

Figure 5 also depicts the *CloudSat* rain-rate  $R_C$  results retrieved from CPR measurements shown in Fig. 1. To closely match the WSR-88D retrievals,  $R_C$  data depicted in Fig. 5 represent average values for the rain layer resolved by the ground-based radar measurements. The CPR data that were suspected to be contaminated by surface returns were not used in the retrievals. The *CloudSat* results are shown for the same latitude interval as the KGWX rain-rate estimates.

As seen from Fig. 5, the collocated WSR-88D and CPR retrievals of rain rate are in overall agreement, except for a small area of warm rain observed to the

south of  $33^\circ$ . The rainfall echo in this area does not generally extend above the freezing level, and therefore no radar BB signatures are present. Overall, results for both ground-based and satellite retrieval exhibit characteristic maxima of rain rates in the regions of isolated convective activity. Some underestimation of *CloudSat* retrievals relative to the ground-based estimates is present for the highest rain-rate peak (i.e., near  $33.25^\circ$ ), which corresponds to the squall line seen to the south from the KGWX radar site in Fig. 2 and is slightly mismatched in satellite and ground-based data.

#### 4. Statistical results of intercomparisons

The intercomparison data from all 12 aforementioned precipitation events of collocated WSR-88D (including KGWX and KSHV) and CPR rain-rate retrievals are shown on a scatterplot in Fig. 6a. The presented data correspond to the rainfall exhibiting the BB as detected by the *CloudSat* measurements. The  $Z_e$ - $R$  relation in (1) was used for WSR-88D retrievals. Although most such rainfall can be considered to be stratiform, some local areas of convective-rain elevated BB features may be present as discussed in the analysis of Fig. 1.

To assess intercomparisons of rain-rate retrievals in a quantitative sense, the correlation coefficient  $r$  between  $R_C$  and  $R_N$  as well as different statistical parameters characterizing the retrieval intercomparisons were calculated. These statistical parameters include the normalized relative mean bias (RMB),

$$\text{RMB} = \langle (R_C - R_N) \rangle \times \langle R_N \rangle^{-1} \times 100\%, \quad (5)$$

the root-mean-square error (RMSE),

$$\text{RMSE} = \langle (R_C - R_N)^2 \rangle^{0.5}, \quad (6)$$

and the normalized mean absolute difference (NMAD),

$$\text{NMAD} = \langle |R_C - R_N| \rangle \times \langle R_N \rangle^{-1} \times 100\%, \quad (7)$$

where angle brackets denote averaging with respect to the dataset, which, for all of the events considered in this study, consisted of 1349 closely collocated ground-based and satellite rain-rate estimates.

Table 1 presents the statistical parameters of the ground-based and spaceborne rain-rate retrievals for the 12 individual events and for the whole dataset, the scatterplots of which are shown in Fig. 6. There is a relatively good average correlation between  $R_N$  and  $R_C$  values, which is characterized by a correlation coefficient of 0.67 for the whole dataset. On average, the *CloudSat* estimates are biased slightly positive (higher;

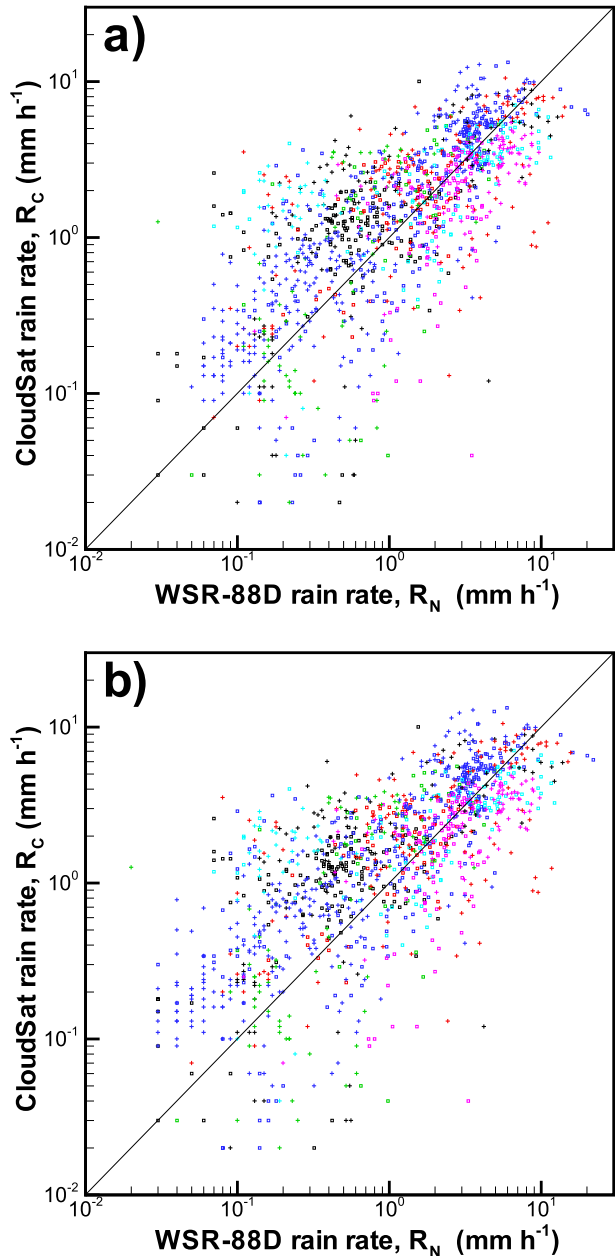


FIG. 6. The scatterplots between approximately collocated rain-rate retrievals from the *CloudSat* CPR and KGWX/KSHV radar measurements for the (a)  $Z_e = 200R^{1.6}$  and (b)  $Z_e = 300R^{1.4}$  relations. Combined data from 12 observational events are shown. Black, red, green, blue, cyan, and purple square/plus symbols correspond to the first, second, third, fourth, fifth, and sixth KGWX/KSHV events as marked in Table 1.

~10%) in comparison with the WSR-88D retrievals. The NMAD value of 58% for the whole dataset is comparable to estimated uncertainties of retrievals. As with *CloudSat* retrievals, reflectivity-based WSR-88D rain-rate retrievals also have substantial errors. Krajewski et al. (2010) showed that these errors for event total

accumulations are on the order of 25%–40%. Higher errors are expected for WSR-88D instantaneous rain-rate retrievals, which are compared here with satellite retrievals.

An analysis of the statistical scores for individual events (Table 1) shows that larger *CloudSat* rain-rate biases (relative to the WSR-88D retrievals) are observed for those events characterized by lighter rainfall with mean  $R_C \leq 2 \text{ mm h}^{-1}$ . One possible reason for this fact is that, as mentioned previously, the uncertainty of the CPR gradient method retrievals degrades as rain rate diminishes and signal attenuation in rain becomes less pronounced. For the rest of the events with mean  $R_C > 2 \text{ mm h}^{-1}$ , the relative biases between satellite- and ground-based radar rain-rate estimates are generally within  $\pm 34\%$ . These results are consistent with previous comparisons between *CloudSat* and WSR-88D rain-rate estimates in landfalling Hurricanes Gustav and Ike, which were characterized by relative biases in the range from  $-8\%$  to  $31\%$  and standard deviations of  $\sim 54\%$ – $56\%$  (Matrosov 2011).

Overall, it can be concluded that the *CloudSat*–WSR-88D retrieval differences are within uncertainties caused by joint errors of ground-based and satellite remote sensing approaches, because the variance of the difference between two independent estimates of rain rate is the sum of their variances and the variance can be considered as the expected error (which is defined in terms of the standard deviation) squared.

Although, for the purpose of intercomparison consistency, the results in Table 1 and Figs. 5 and 6a were obtained using the WSR-88D retrievals utilizing the relation in (1), an effect of using another common NEXRAD  $Z_e$ – $R$  relation, namely,

$$Z_e = 300R^{1.4}, \quad (8)$$

was evaluated. Even though the relation in (8) is considered to be convective in the NMQ system (e.g., Zhang et al. 2011), it is sometimes used as a default relation in many WSR-88D-based QPE schemes. A scatterplot of spaceborne and ground-based radar rain-rate retrievals when (8) was used for deriving WSR-88D estimates is shown in Fig. 6b. This change of the  $Z_e$ – $R$  relation did not significantly affect intercomparison results. The corresponding statistical scores for the whole dataset were 0.66, 15%,  $2.0 \text{ mm h}^{-1}$ , and 61% for  $r$ , RMB, RMSE, and NMAD, respectively, which are relatively close to the scores for the WSR-88D relation in (1) that are given in the first line of Table 1.

There is not much difference between the results when either (1) or (8) is used, even though the overwhelming majority of retrievals in this study represent

stratiform precipitation regions with low-to-moderate rain rates. This is because both stratiform and convective default NEXRAD  $Z_e$ – $R$  relations produce very similar ( $\sim 10\%$ – $15\%$ ) rain rates when reflectivities are within the range between 25 and 45 dBZ. This was a typical range of WSR-88D reflectivities that were observed during the observational events considered in this study.

The  $Z_e$ – $R$  relations are determined by the raindrop size distributions (DSDs). While there is not much difference in the intercomparisons resulting from the choice between the WSR-88D mean relations in (1) and (8), the variability among such relations for individual events that is due to DSD differences can be significant (e.g., Doviak and Zrnicek 1993). The DSD-driven variability in *CloudSat*  $\alpha$ – $R$  relations used for the satellite retrievals here is expected to be more modest (in relative terms) than that for S-band  $Z_e$ – $R$  relations because of significant non-Rayleigh-scattering effects that dampen the DSD influence at W band. It is suggested that the varying biases between ground-based and satellite radar retrievals of rain rate for different events are caused, in part, by DSD-induced differences in event-specific  $Z_e$ – $R$  and  $\alpha$ – $R$  relations. Specific DSDs and relations, however, are typically not known a priori for particular events, and the radar-based methods usually use mean  $Z_e$ – $R$  relations as presented in this study.

The *CloudSat* gradient rain-rate retrieval method is immune to the CPR absolute calibration, but WSR-88D reflectivity-based QPE retrievals are sensitive to the reflectivity measurement errors. Although the NEXRAD radars undergo regular absolute calibration checks, some calibration biases are possible (e.g., Gourley et al. 2003). A 1-dB bias in  $Z_e$  measurements, for example, would result in an  $\sim 15\%$ – $20\%$  shift in retrieved rain rates when a  $Z_e$ – $R$  relation with an exponent similar to those in (1) and (8) is used. This will affect statistical parameters of intercomparisons (except for the correlation coefficient). The detailed calibration analysis of the WSR-88Ds is, however, beyond the scope of the current research. The standard quality-controlled level-II NEXRAD data were used in this study.

Another potential factor that can negatively affect the WSR-88D reflectivity-based rain-rate retrievals is partial beam blockage, which could result in underestimation of reflectivity values and, hence, reduce rain rates retrieved from ground-based radar data. The lower beam edge of the lowest elevation tilt for NEXRAD scanning routines is close to  $0^\circ$  and shielding by nearby tall terrain features or objects can cause partial beam blockage for some azimuthal directions. Although the KGWX and KSHV radar coverage maps from the National Climatic Data Center (obtained online from

<http://www.ncdc.noaa.gov/nexradinv/>) do not indicate any significant beam blockage even for the lowest beam tilt at these radar locations, influences of potential beam-blockage effects on the derived rain-rate retrieval intercomparison statistics were evaluated as part of this study.

During this evaluation, in addition to the intercomparisons described above when data from all WSR-88D tilts were used, the intercomparisons of spaceborne and ground-based radar rain retrievals were conducted with WSR-88D data when the  $0.5^\circ$  elevation tilt data were excluded. As a result of this exclusion, the RMB, RMSE, NMAD, and  $r$  values corresponding to the  $Z_e$ - $R$  relation in (1) and the whole dataset changed to 19%,  $2.2 \text{ mm h}^{-1}$ , 67%, and 0.6, respectively. Similar relative changes were present when the  $Z_e$ - $R$  relation in (8) was used (data are not shown). The overall change in statistical scores is relatively modest, and their variability may also (i.e., in addition to potential beam-blockage effects) be influenced by some vertical variability in rain rates because the data at lower altitudes were omitted as a result of the exclusion of the lowest tilt measurements. Thus it can be concluded that the WSR-88D partial beam-blockage effect (if any) did not influence the results of this study intercomparison in a significant way.

## 5. Summary and conclusions

Attenuation-based approaches to retrieve rain rates over water surfaces have been used with the *CloudSat* spaceborne 94-GHz radar measurements for a number of years, and the corresponding data products exist. This study was focused on evaluating *CloudSat* experimental retrievals of rain rates over land surfaces using reflectivity gradients observed in liquid hydrometeor layers of predominantly stratiform precipitating systems exhibiting radar bright band. The evaluation was achieved by intercomparisons of *CloudSat* rain-rate retrievals with conventional estimates from WSR-88Ds using data collected during 2006–12 from satellite overpasses in the vicinity of the WSR-88D sites.

The WSR-88D KGWX and KSHV radars were chosen for these intercomparisons because of the existence of *CloudSat* overpasses over them during precipitation events and also because of the relatively flat terrain in their vicinity, which minimizes beam-blockage effects in ground-based radar measurements. Rain-rate retrievals using the *CloudSat* attenuation-based reflectivity-gradient method were compared with estimates from the KGWX and KSHV radars that are closely collocated in space and time. The standard NEXRAD QPE approach, which is based on utilizing the  $Z_e$ - $R$  relations, was used in these intercomparisons. This approach is widely used

in many hydrological and meteorological applications, and it was considered in this study as a reference for testing a relatively novel satellite technique such as the *CloudSat* rain-rate retrieval method over land. The rain-rate retrievals from the satellite and ground-based radars used in this study were performed for rainfall layers that were free from contamination from melting and ice hydrometeors. The BB and CPR surface return requirements limited retrieval datasets to events with freezing levels that were not lower than approximately 2 km above radar sites.

The intercomparison results showed that rain rates obtained from *CloudSat* and WSR-88D measurements generally were in good agreement. Depending on the choice of the WSR-88D relation and the radar tilts used, correlation coefficients for the whole dataset consisting of 12 observational events were in a range between 0.6 and 0.67. The satellite retrievals were biased on average by about 10%–20% higher (positive) relative to ground-based radar estimates; for individual events with mean rain rates exceeding about  $2 \text{ mm h}^{-1}$ , the biases were within  $\pm 34\%$ . Events with lighter rainfall generally exhibited higher biases and lower correlations, in part because of larger satellite-retrieval uncertainties. The normalized mean absolute differences between satellite and ground-based retrievals were on average  $\sim 60\%$ . These differences are on the order of magnitude of joint rain-rate retrieval uncertainties from both the ground-based and satellite remote sensing approaches. Estimating potential partial beam-blockage effects on the ground-based radar measurements in the dataset considered in this study indicated that these effects (if present) were not likely to significantly change the results.

Although the majority of the compared rain-rate data corresponded to stratiform rainfall regime with a stable radar BB, rainfall peaks associated with isolated convective regions were also identified by *CloudSat*, and a reasonable agreement was present between WSR-88D and *CloudSat* rain-rate retrievals in these regions. Spaceborne retrievals for isolated regions of warm rain were not very favorable when compared with ground-based radar data, which might indicate limitations of the *CloudSat* reflectivity-gradient method for this type of rainfall. The intercomparison results are encouraging for the use of the *CloudSat* gradient method over land surfaces, but in the future more intercomparisons are needed with a larger variety of sensors to better understand accuracy and limitations of this method in precipitation of various types. A comparison of ground-based and satellite radar data reveals that WSR-88Ds observe ice regions of stratiform precipitating systems well. It would be useful in future to evaluate whether operational weather radars can provide reliable quantitative

information on ice contents in such stratiform systems using simple approaches that are based on reflectivity data (e.g., Matrosov 1997).

*Acknowledgments.* This study was funded in part by NASA Project NNX13AQ31G and the NOAA Hydrometeorology Testbed Project.

#### REFERENCES

- Battaglia, A., J. Haynes, T. L'Ecuyer, and C. Simmer, 2008: Identifying multiple-scattering-affected profiles in *CloudSat* observations over the oceans. *J. Geophys. Res.*, **113**, D00A17, doi:10.1029/2008JD009960.
- , S. Tanelli, S. Kobayashi, D. Zrnica, R. J. Hogan, and C. Simmer, 2010: Multiple scattering in radar systems: A review. *J. Quant. Spectrosc. Radiat. Transfer*, **111**, 917–947, doi:10.1016/j.jqsrt.2009.11.024.
- Bringi, V. N., and V. Chandrasekar, 2001: *Polarimetric Doppler Weather Radar*. Cambridge University Press, 636 pp.
- Doviak, R. J., and D. S. Zrnica, 1993: *Doppler Radar and Weather Observations*. Academic Press, 562 pp.
- Gourley, J. J., B. Kaney, and R. A. Maddox, 2003: Evaluating the calibrations of radars: A software approach. *31st Int. Conf. on Radar Meteorology*, Seattle, WA, Amer. Meteor. Soc., P3C.1. [Available online at <https://ams.confex.com/ams/pdfpapers/64171.pdf>.]
- Haynes, J. M., T. S. L'Ecuyer, G. L. Stephens, S. D. Miller, C. Mitrescu, N. B. Wood, and S. Tanelli, 2009: Rainfall retrieval over the ocean with spaceborne W-band radar. *J. Geophys. Res.*, **114**, D00A22, doi:10.1029/2008JD009973.
- Hudak, D., P. Rodriguez, and N. Donaldson, 2008: Validation of the *CloudSat* precipitation occurrence algorithm using the Canadian C band radar network. *J. Geophys. Res.*, **113**, D00A07, doi:10.1029/2008JD009992.
- Krajewski, W. F., G. Villarni, and J. A. Smith, 2010: Radar-rainfall uncertainties: Where are we after thirty years of effort? *Bull. Amer. Meteor. Soc.*, **91**, 87–94, doi:10.1175/2009BAMS2747.1.
- Lebsack, M. D., and T. S. L'Ecuyer, 2011: The retrieval of warm rain from *CloudSat*. *J. Geophys. Res.*, **116**, D20209, doi:10.1029/2011JD016076.
- Matrosov, S. Y., 1997: Variability of microphysical parameters in high-altitude ice clouds: Results of the remote sensing method. *J. Appl. Meteor.*, **36**, 633–648, doi:10.1175/1520-0450-36.6.633.
- , 2007: Potential for attenuation-based estimations of rainfall rate from *CloudSat*. *Geophys. Res. Lett.*, **34**, L05817, doi:10.1029/2006GL029161.
- , 2008: Assessment of radar signal attenuation caused by the melting hydrometeor layer. *IEEE Trans. Geosci. Remote Sens.*, **46**, 1039–1047, doi:10.1109/TGRS.2008.915757.
- , 2011: *CloudSat* measurements of landfalling Hurricanes Gustav and Ike (2008). *J. Geophys. Res.*, **116**, D01203, doi:10.1029/2010JD014506.
- , 2013: Characteristics of landfalling atmospheric rivers inferred from satellite observations over the eastern North Pacific Ocean. *Mon. Wea. Rev.*, **141**, 3757–3768, doi:10.1175/MWR-D-12-00324.1.
- , A. Battaglia, and P. Rodriguez, 2008: Effects of multiple scattering on attenuation-based retrievals of stratiform rainfall from *CloudSat*. *J. Atmos. Oceanic Technol.*, **25**, 2199–2208, doi:10.1175/2008JTECHA1095.1.
- Mitrescu, C., T. L'Ecuyer, J. Haynes, S. Miller, and J. Turk, 2010: *CloudSat* precipitation profiling algorithm—Model description. *J. Appl. Meteor. Climatol.*, **49**, 991–1003, doi:10.1175/2009JAMC2181.1.
- Sassen, K., S. Matrosov, and J. Campbell, 2007: *CloudSat* spaceborne 94 GHz radar bright bands in the melting layer: An attenuation-driven upside-down lidar analog. *Geophys. Res. Lett.*, **34**, L16818, doi:10.1029/2007GL030291.
- Stephens, G. L., and Coauthors, 2008: *CloudSat* mission: Performance and early science after the first year of operation. *J. Geophys. Res.*, **113**, D00A18, doi:10.1029/2008JD009982.
- Tanelli, S., S. L. Durden, E. Im, K. S. Pak, D. G. Reinke, P. Partain, J. M. Haynes, and R. Marchand, 2008: *CloudSat's* cloud profiling radar after two years in orbit: Performance, calibration, and processing. *IEEE Trans. Geosci. Remote Sens.*, **46**, 3560–3573, doi:10.1109/TGRS.2008.2002030.
- Zhang, J., and Coauthors, 2011: National Mosaic and Multi-Sensor QPE (NMQ) System: Description, results, and future plans. *Bull. Amer. Meteor. Soc.*, **92**, 1321–1338, doi:10.1175/2011BAMS-D-11-00047.1.